Int. J. Electrochem. Sci., 15 **(2020)** 1742 – 1756, doi: 10.20964/2020.02.55

International Journal of
ELECTROCHEMICAL
SCIENCE
www.electrochemsci.org

Polyaniline/Ba bismuthate Nanobelts for Sensitive Electrochemical Detection of Tartaric Acid

H. J. Chen[1], F. F. Lin[1], C. H. Yu[1], Z. Y. Xue[1], Z. Wang[1], L. Z. Pei[1,], H. Wu[1], P. X. Wang[1], Q. M. Cong[1], C. G. Fan[1], and X. Z. Ling[2,3,*]*

[1] School of Materials Science and Engineering, Anhui University of Technology, Ma'anshan, Anhui 243002, P. R. China
[2] School of Civil Engineering, Harbin Institute of Technology, Heilongjiang, Harbin 150090, P. R. China
[3] School of Civil Engineering, Qingdao Technological University, Shandong, Qingdao 266520, P. R. China
[*]E-mail: lzpei1977@163.com (L. Z. Pei), ling_xianzhang@163.com (X. Z. Ling),

Received: 1 October 2019 / *Accepted:* 1 December 2019 / *Published:* 31 December 2019

An *in-situ* polymerization route has been applied to obtain polyaniline/Ba bismuthate nanobelt (PAn/BBN) composites with different polyaniline mass percentage. The PAn/BBN composites were characterized by X-ray diffraction (XRD), transmission electron microscopy (TEM), high-resolution TEM (HRTEM) and electrochemical cyclic voltammetry (CV) method. XRD shows that the obtained composites are composed of monoclinic $BaBiO_{2.5}$ phase. Transmission electron microscopy observations show that the amorphous polyaniline particles with the size of less than 100 nm attach to the surface of the Ba bismuthate nanobelts. The PAn/BBN composites modified glassy carbon electrode (GCE) exhibits good electro-catalytic activity toward tartaric acid (TA). A pair of quasi-reversible CV peaks are located at -0.69 V and +0.49 V, respectively. The negative shift and increase in the current show that the PAn/BBN composites modified GCE has enhanced electro-catalytic activity toward TA. The influence of the scan rate and electrolyte on the electrochemical responses has also been researched. The limit of detection (LOD) decreases from 0.12 μM to 0.08 μM with increasing the polyaniline mass percentage from 10% to 40%. The PAn/BBN composites modified GCE shows good stability and reproducibility.

Keywords: Ba bismuthate nanobelts, Polyaniline, Transmission electron microscopy, Electrochemical detection, Tartaric acid.

1. INTRODUCTION

Bi-based materials exhibited good application potential in electrochemical devices owing to their good electrochemical performance [1-3]. For example, ammonium tetrafluorobismuthate (BiF_4-

CPE) modified carbon paste electrode was developed for the electrochemical detection of heavy metal ions by anodic stripping voltammetric method [4]. The BiF_4-CPE revealed a favorable performance for the electrochemical determination of Cd (II) and Pb (II) in acidic solution (pH=0.5-2.5) in the presence of dissolved oxygen at μg L^{-1} concentration level. Bi nanoscale particles/porous carbon on graphene sheets were reported to be used as efficient materials for the electrochemical detection of heavy metal ions [5]. Bismuthate nanoscale materials, such as $ZnBi_{38}O_{60}$ nanobundles [6], zinc bismuthate nanorods [7], aluminium bismuthate nanorods [8] and bismuth tellurate nanospheres [9] could be used as the glassy carbon electrode (GCE) modified materials for effective determination of 4-nitrophenol, *L*-Cysteine and tartaric acid (TA), respectively with low limit of detection (LOD) and wide linear range.

Among these Bi-based materials, Ba bismuthate nanobelts are expected to possess good electro-catalytic performance for the detection of biological molecules. In our previous research, Ba bismuthate nanobelts were obtained by a simple hydrothermal process and exhibited good electro-catalytic performance for TA detection in neutral solution [10]. The LOD was 0.12 μM and linear detection range was 0.001-2 mM. TA is used in the food field and chemical industry, and it is important to detect TA in liquid food, such as fruits or fruit products for assessing the quality of the liquid food and assuring human health [11,12]. Cobalt(II)-phthalocyanine modified carbon paste electrode was also reported for the electrochemical detection of TA with the LOD and linear range of 7.29 μM and 0.01-0.1 mM, respectively [13]. However, in fact, the electrochemical detection performance for TA, such as LOD is still expected to be improved for accurate determination of TA in real liquid samples.

The electrochemical activity of the electrode materials can be obviously enhanced by forming the nanoscale composites [14-17]. Polyaniline is a kind of important polymer which exhibits good electrochemically active performance, electrical conductivity and thermal stability [18,19]. It has been confirmed that the electrochemical performance of the nanocomposites with polyaniline and nanoscale materials can be greatly enhanced, such as graphene nanosheets/polyaniline nanofibers composites [20], single-walled carbon nanotube with polyaniline composites [21], hierarchical porous carbon/polyaniline composites [22] and molybdenum disulfide nanosheets-polyaniline composites [23]. Ba bismuthate nanobelts exhibited good electrochemical performance for TA detection. It is expected that the electrochemical performance of the Ba bismuthate nanobelts may be improved by combining the polyaniline.

In-situ polymerization route is an effective method for the formation of the composites with polymers and nanoscale materials [24-27]. In this work, Ba bismuthate nanobelts were combined with polyaniline with different contents to form polyaniline/Ba bismuthate nanobelt composites by *in-situ* polymerization route. The polyaniline/Ba bismuthate nanobelt composites were applied as the GCE modified materials for the electrochemical detection of TA. The roles of the influential factors (including TA concentration, scan rate, electrolytes and polyaniline content) on the electrochemical responses of TA at the composites modified GCE were analyzed in detail by cyclic voltammetry (CV) method. The polyaniline/Ba bismuthate nanobelt composites modified GCE shows improved electrochemical activity toward TA.

2. EXPERIMENTAL PROCEDURE

Ba bismuthate nanobelts were obtained by a simple hydrothermal route which was described elsewhere [10]. Methenyl trichloride, iron trichloride, ethanol and aniline are of analytical grade and purchased from Sinopharm Chemical Reagent Co., Ltd. of P. R. China. Distilled water was used during the experimental procedure.

Ba bismuthate nanobelts with definite mass were dispersed into 20 mL methenyl trichloride solution. Then aniline monomer with definite mass was added into 20 mL methenyl trichloride with Ba bismuthate nanobelts under continous stirring. The mass ratio of the aniline and Ba bismuthate nanobelts is 1:9, 2:8 and 4:6, respectively. After the stirring for 30 min, iron trichloride and aniline were added into the methenyl trichloride solution with sonicating. The molar ratio of the aniline and iron trichloride was 5:12. The reaction lasted for 3 h at 0 to 5 ℃ under the sonicating. The obtained products were filtered and washed using distilled water and ethanol, respectively. Finally the composite were dried at 80 ℃ under vacuum. The obtained polyaniline/Ba bismuthate nanobelts with the mass percentage of 10%, 20% and 40% were abbreviated as PAn/BBNs-10wt.%, PAn/BBNs-20wt.% and PAn/BBNs-40wt.%, respectively.

The phase of the samples was analyzed by X-ray diffraction (XRD) (Bruker AXS D8, Germany) with Cu K_α radiation (λ=1.5406 Å). 2θ scan range was 20° to 80°. For the morphological observation, the samples were observed by transmission electron microscopy (TEM) and high-resolution TEM (HRTEM) using a JEOL JEM-2100 TEM. The composite suspensions were dropped onto the Cu grids coated with a carbon film followed by drying in air.

The bare GCE with the diameter of 3 mm was successively polished using the sand paper with 0.05 μm and cleaned using distilled water and ethanol for several times in the ultrasonic bath. And the treated bare GCE was dried at room temperature. The polyaniline/Ba bismuthate nanobelt composites were dispersed into N-dimethylformamide (DMF) solution for the sonicating treatment of 30 min. A 10 μL polyaniline/Ba bismuthate nanobelt composite suspension was casted to the surface of the bare GCE using a pipette and dried in an infrared lamp.

The obtained PAn/BBNs modified GCE was immersed in the mixed solution of 0.1 M electrolyte and TA with different concentrations. The electrochemical measurements were carried out at room temperature by CV method on a CHI604D electrochemical workstation (Shanghai Chenhua Instrument Co., P. R. China) between -1.0 V~+1.0 V at different scan rate. The conventional three electrode system consisted of PAn/BBNs modified GCE, Pt wire electrode and saturated calomel electrode which acted as the working electrode, auxiliary electrode and reference, respectively.

3. RESULTS AND DISCUSSION

Structural features of the obtained products are characterized by XRD patterns. Figure 1 shows the XRD patterns of the Ba bismuthate nanobelts and PAn/BBNs-20wt.%. The diffraction peaks of the Ba bismuthate nanobelts (Figure 1a) can be well indexed to monoclinic $BaBiO_{2.5}$ (JCPDS card No. 50-0854). The XRD pattern of the PAn/BBNs-20wt.% (Figure 1b) is similar to that of the Ba bismuthate

nanobelts. However, the intensity of the diffraction peaks decreases obviously which may originate from the amorphous polyaniline. The result indicates that the PAn/BBN composites are composed of monoclinic $BaBiO_{2.5}$ phase.

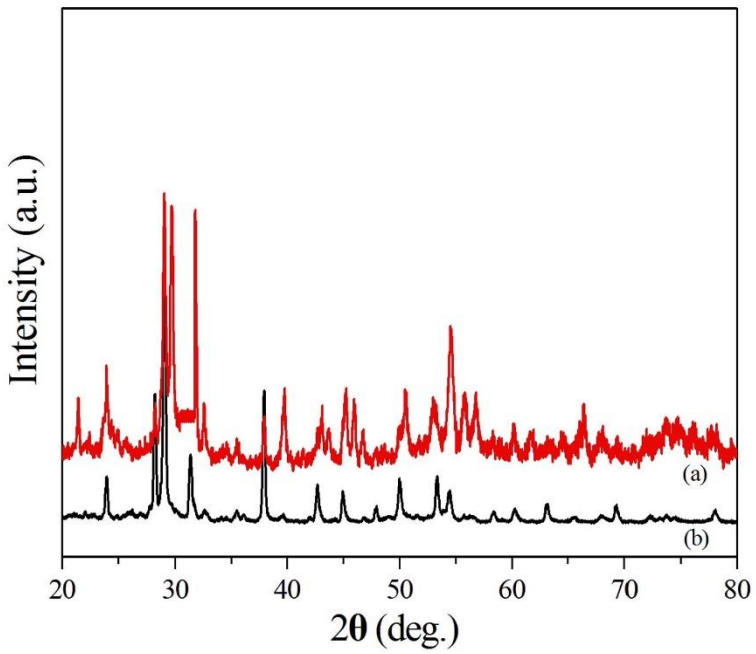

Figure 1. XRD patterns of the Ba bismuthate nanobelts and PAn/BBNs-20wt.%.

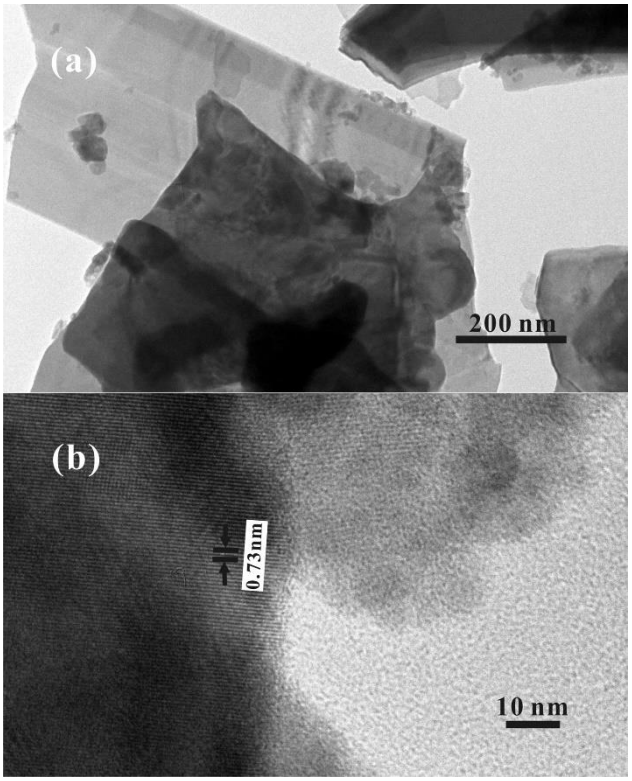

Figure 2. Transmission electron microscopy images of the PAn/BBNs-20wt.%. (a) TEM, (b) HRTEM.

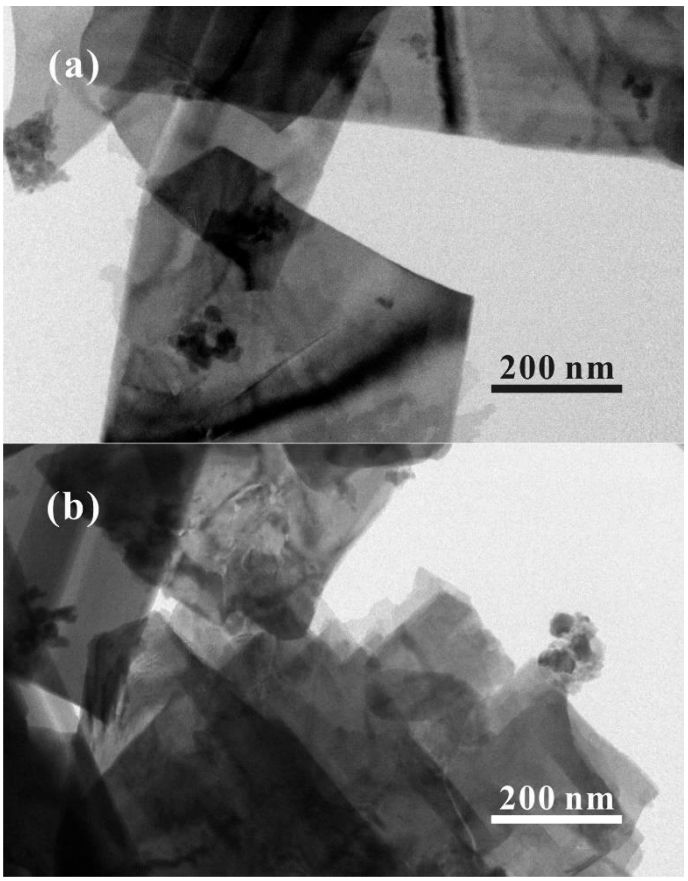

Figure 3. TEM images of the PAn/BBNs with various PAn mass percentage. (a) 10%, (b) 40%.

PAn/BBNs-20wt.% was selected for the morphological analysis of the obtained nanobelt composites. Figure 2 shows the transmission electron microscopy images of the PAn/BBNs-20wt.%. Observed from Figure 2a, the amorphous polyaniline nanoscale particles with the size of less than 100 nm attach to the surface of the Ba bismuthate nanobelts. The thickness of the Ba bismuthate nanobelts is about 30 nm. The higher resolution HRTEM image (Figure 2b) further shows that the amorphous polyaniline particles attach to the surface of the crystalline Ba bismuthate nanobelts. The Ba bismuthate nanobelts have uniform lattice fringes. The interplanar distance of the lattice plane is about 0.73 nm which corresponds to that of {100} crystal planes of monoclinic $BaBiO_{2.5}$. Figure 3 shows the TEM images of the PAn/BBNs with the polyaniline mass percentage of 10% and 40%, respectively. It is obvious that the morphology of the PAn/BBNs with different mass percentage is similar. However, the amount of the polyaniline particles attached at the surface of the Ba bismuthate nanobelts increases obviously with increasing the polyaniline mass percentage from 10% to 40%. The results show that the polyaniline mass percentage has an important role in the amount of the polyaniline particles at the surface of the nanobelts. The combination of the Ba bismuthate nanobelts is similar to that of the nanoscale materials reported by us in our previous research [27-29].

The formation of the polyaniline/Ba bismuthate nanobelt composites is based on *in-situ* oxidative polymerization route. During the *in-situ* polymerization process, aniline and iron trichloride act as the monomer and oxidizing agent, respectively. In the experimental process, iron trichloride was directed added to the aniline solution and methenyl trichloride-containing Ba bismuthate nanobelts and

aniline were sonicated. Aniline monomers were absorbed to the surface of the Ba bismuthate nanobelts. Iron trichloride protonates aniline forming the anilinium cations and radical cations and resulting in the formation of the covalent bonds between the aniline units [30]. Aniline monomers polymerize at the surface of the Ba bismuthate nanobelts leading in the formation of PAn/BBN composites.

Further experiments of cyclic voltammetry were applied in order to analyse the electrochemical activity of the PAn/BBN composites modified GCE toward TA. PAn/BBNs-20wt.% composites were used as the typical GCE modified materials. The electrochemical responses of 2 mM TA in 0.1 M KCl solution at different electrodes are recorded which is shown in Figure 4. As a comparison, the CV of PAn/BBNs-20wt.% modified GCE in 0.1 M KCl solution without TA is also obtained. Observed from Figure 4, it is obvious that bare GCE has no electro-catalytic activity toward TA. PAn/BBNs-20wt.% modified GCE has also no electro-catalytic activity in KCl solution. A pair of electrochemical CV peaks are observed using BBNs and PAn/BBNs-20wt.% modified GCEs in the mixed solution of 2 mM TA and 0.1 M KCl. The potential of the CV peaks for cvp1 and cvp1′ is -0.49 V and +0.01 V, respectively at the BBNs modified GCE. The current is 94.4 μA and 65.6 μA for cvp1 and cvp1′, respectively. However, the potential of the CV peaks at the PAn/BBNs-20wt.% modified GCE shifts to -0.69 V and +0.49 V for cvp1 and cvp1′, respectively.

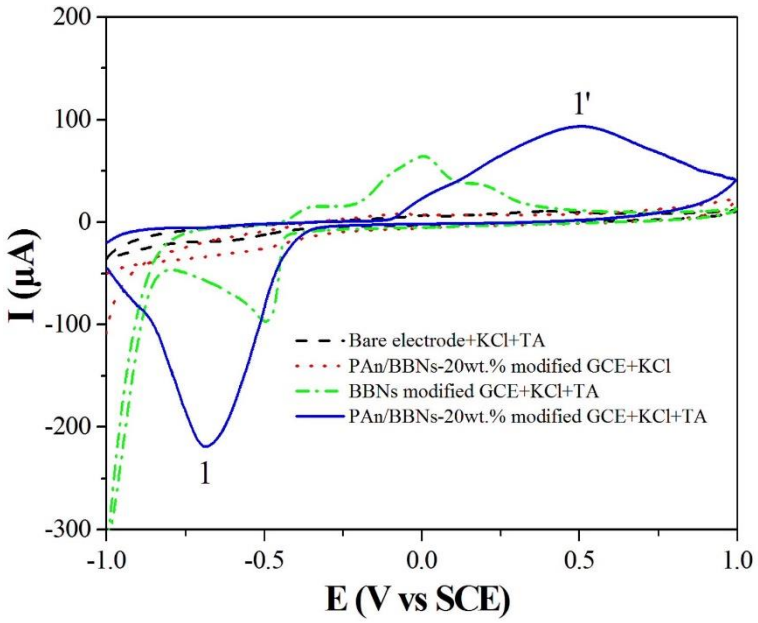

Figure 4. CVs of bare GCE, BBNs and PAn/BBNs-20wt.% modified GCEs in 0.1 M KCl solution with 2 mM TA and PAn/BBNs-20wt.% modified GCE in 0.1 KCl solution without TA using the scan rate of 50 mVs^{-1}.

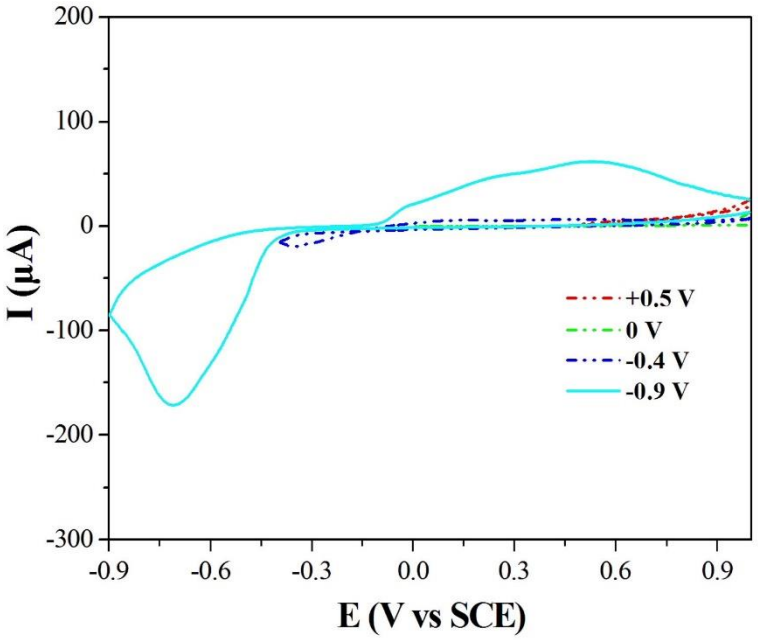

Figure 5. The CVs of 2 mM TA in 0.1 M KCl solution at the PAn/BBNs-20wt.% modified GCE using different initial scan potential. Scan rate, 50 mVs^{-1}.

The potential of cvp1 shifts to more negative direction. And the current increases to 220.3 μA and 93.3 μA for cvp1 and cvp1′, respectively. Comparing the bare GCE which has a CV peak at -0.49 V for cvp1, the potential at the PAn/BBNs-20wt.% modified GCE shows 200 mV negative shift. The Al bismuthate nanorods modified GCE showed a pair of semi-reversible electrochemical CV peaks at -0.08 V and -0.53 V, respectively in 2 mM TA and 0.1 M KCl solution [8]. An irreversible electrochemical CV peak located at +1.15 V was observed at the cobalt(II)-phthalocyanine modified carbon paste electrode in 4 mM TA and 0.05 M acetic acid/acetate buffer solution with pH = 4.5 [12]. β-Cyclodextrin (CD)-carbon nanotubes (CNTs) modified GCE showed a pair of CV peaks at -0.32 V and -0.18 V, respectively in 10 mM TA and 10 M pbs (pH=6.0) solution [31]. Using the Cu bismuthate nanoflakes as the GCE modified materials, a pair of semi-reversible electrochemical CV peaks were located at -0.45 V and -0.02 V in 0.1 M KCl and 2 mM TA solution [32]. Compared with above results, the PAn/BBNs-20wt.% modified GCE shows negative shift in the potential of the CV peaks. The negative shift and increase in the current show that the PAn/BBNs modified GCE has enhanced electro-catalytic activity toward TA, which provides a great approach for TA determination. The enhanced electro-catalytic activity toward TA may be attributed to the polyaniline and synergistic role between the polyaniline and Ba bismuthate nanobelts. The large specific surface area of the PAn/BBN composites modified GCE may offer more adsorption sites improving the electro-catalytic responses and transmission of response signals. Different peak current of the anodic and cathodic CV peaks shows that the electrochemical process at the PAn/BBNs modified GCE belongs to quasi-reversible process.

Figure 5 shows the CVs of 2 mM TA in 0.1 M KCl solution at the PAn/BBNs-20wt.% modified GCE using various initial scan potentials in order to analyse the redox process. No electrochemical signals occur when the initial scan potential is +0.5 V, 0 V and -0.4 V, respectively which is higher than

cvp1 of -0.69 V. When initial scan potential decreases to -0.9 V which is smaller than +0.04 V of cvp1′, a pair of electrochemical CV peaks are produced. The results indicate that cvp1′ is produced from cvp1. Therefore, the obtained electrochemical CV peaks belong to quasi-reversible electrochemical process. TA is a kind of polyoxometalate with coordination role to metal ions and interactions may occur at the surface of the PAn/BBN composites. TA is considered to be oxidized to tartrate at the PAn/BBNs modified GCE [10]. Similar to the electrochemical process at the PAn/BBNs modified GCE, the electrochemical peaks cvp1 and cvp1′ are also attributed to the oxidation and reduction process between TA and tartrate.

The role of the electrolytes on the electrochemical responses of TA has been analyzed by measuring the CVs of 2 mM TA in 0.1 M KCl solution at the PAn/BBN composites modified GCE. Figure 6 shows the CVs of 2 mM TA in different electrolytes with different pH values. The electrochemical responses of 2 mM TA in 0.1 M KBr solution at the composites modified GCE (Figure 6a) is similar to that in KCl solution. Only slight difference occurs in the peak potential and current. No electrochemical CV peaks are observed from the CV in the NaOH solution (pH=12) (Figure 6b). TA and NaOH react to form sodium tartrate in NaOH solution retarding the electrochemical reaction at the PAn/BBNs modified GCE. In CH_3COONa-CH_3COOH (pH=5) (Figure 6c) and H_2SO_4 (pH=2) (Figure 6d) electrolyte, the intensity of the CV peaks at the PAn/BBNs modified GCE increases. Obviously, hydrogen ions promote the electrochemical reaction between TA and tartrate at the PAn/BBNs modified GCE leading to higher electro-catalytic activity.

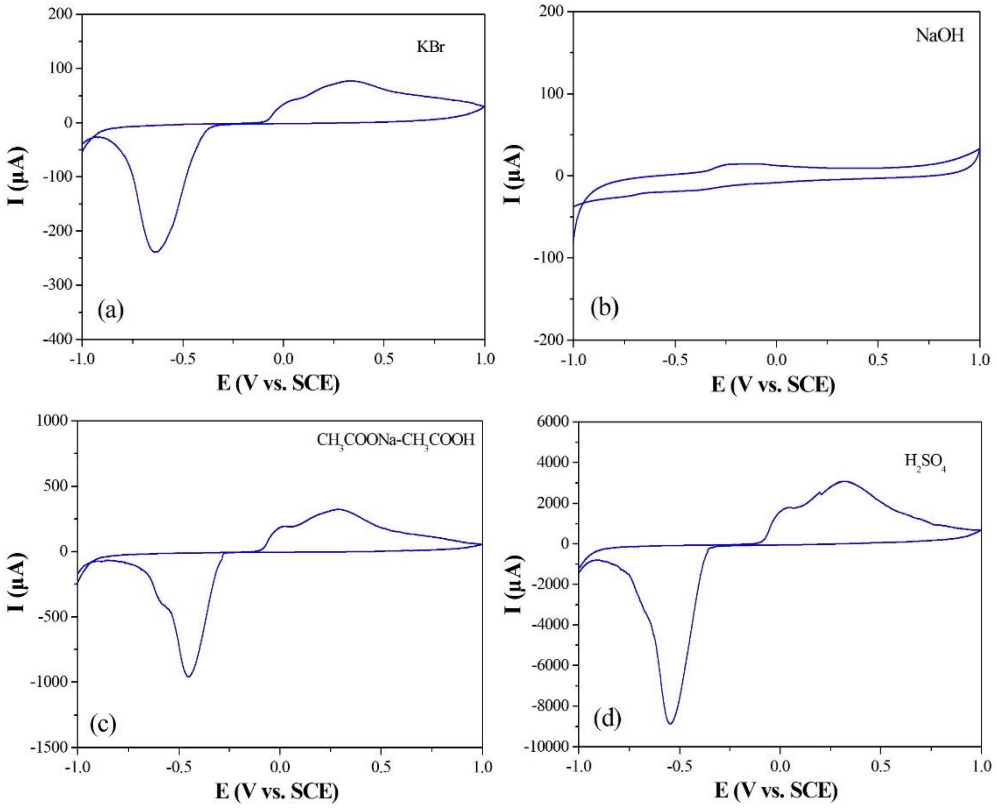

Figure 6. CVs of 2 mM TA at the PAn/BBNs-20wt.% modified GCE in 0.1 M electrolyte with different species using the scan rate of 50 mVs^{-1}. (a) KBr, (b) NaOH, (c) CH_3COONa-CH_3COOH, (d) H_2SO_4.

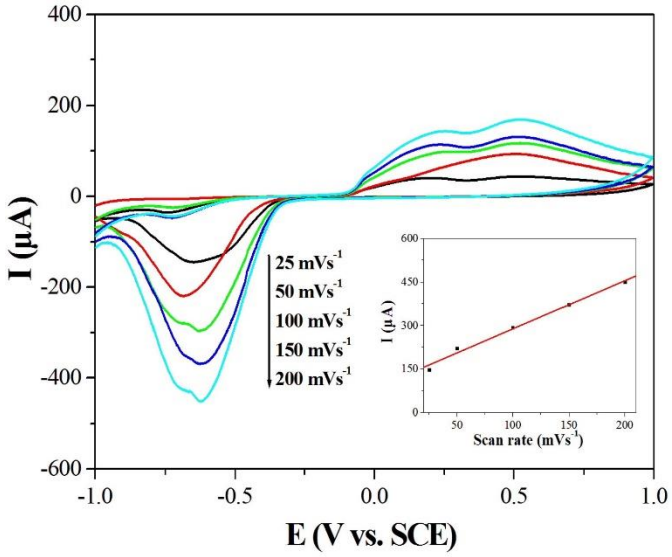

Figure 7. CVs of 2 mM TA in 0.1 M KCl solution at the PAn/BBNs-20wt.% modified GCE using various scan rates. The inset in the bottom-right part is the plot of the current of the CV peak against the scan rate.

Subsequently, to analyze the relationship between the peak current and scan rate, Figure 7 shows the cyclic voltammetric performance for 2 mM TA at the PAn/BBNs-20wt.% modified GCE using different scan rates in 0.1 M KCl solution. The plot of the CV peak current and scan rate is shown in the bottom-right part of Figure 7. The cvp1 peak current increases from 148.33 μA to 450.32 μA with the scan rate increasing from 25 $mV \cdot s^{-1}$ to 200 $mV \cdot s^{-1}$. The plot of the CV peak current and scan rate shows a straight line at different rates from 25 $mV \cdot s^{-1}$ to 200 $mV \cdot s^{-1}$. The result shows that the electrochemical process at the PAn/BBN composites modified GCE belongs to an adsorption-controlled process which is similar to that reported by other groups [12,31,32].

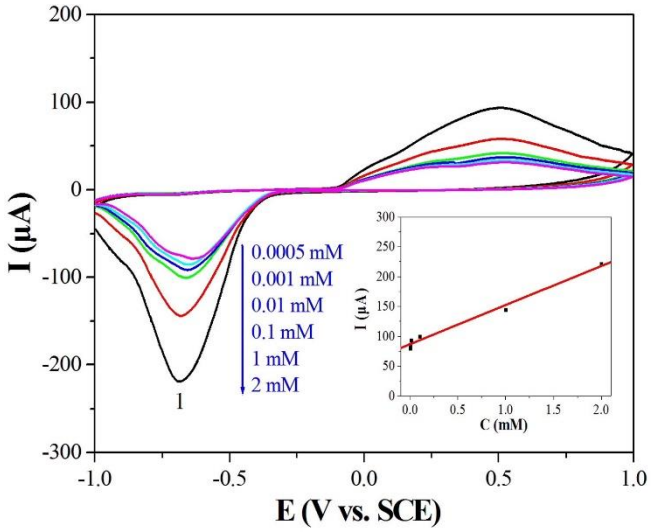

Figure 8. CVs of TA with various concentrations in 0.1 M KCl solution at the PAn/BBNs-20wt.% modified GCE with the scan rate of 50 mVs^{-1}. The inset in the bottom-right part is the plot of the current of the CV peak against TA concentration.

Figure 8 shows the electrochemical CVs after consecutive addition of different concentrations of TA at the PAn/BBNs-20wt.% modified GCE. Clearly, the inset in the bottom-right part of Figure 8 shows that the electrochemical response increases linearly with TA concentration. The PAn/BBNs-20wt.% modified GCE exhibits a linear range of 0.0005-2 mM. The LOD is found to be 0.09 μM. The analytical data of TA using PAn/BBNs-20wt.% modified GCE are listed in Table 1. The correlation coefficient R is 0.993.

Table 1. Analytical data of TA at the PAn/BBNs-20wt.% modified GCE.

CV peak	Regression equation[a]	Correlation coefficient (R)	Linear range (mM)	LOD (μM) [b]
Cvp1	I_p=91.263+65.045C	0.993	0.0005-2	0.09

[a] Where I_p and C refer to the current (μA) and TA concentration (mM)
[b] LOD was analyzed using S/N= 3

The stability and reproducibility of the PAn/BBNs modified GCE were also investigated by CV method in the presence of 2 mM TA in 0.1 M KCl solution.

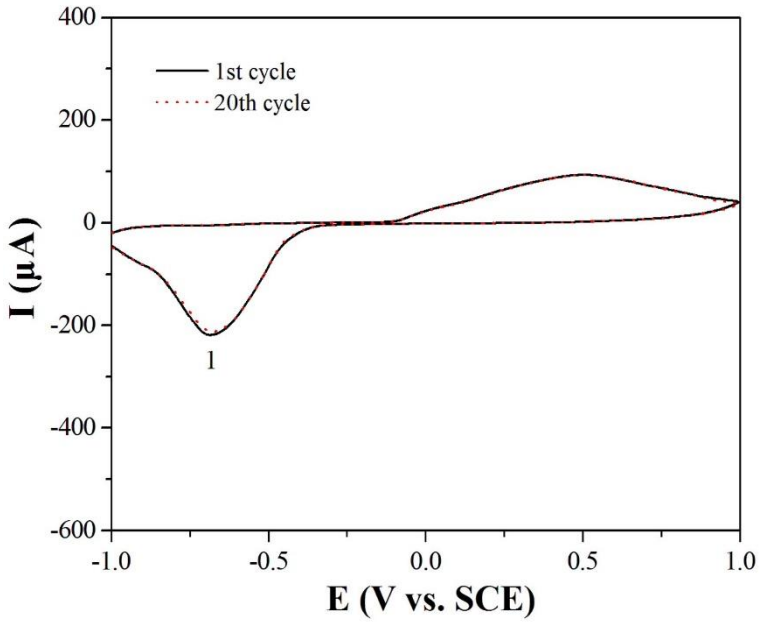

Figure 9. CVs of 2 mM TA in 0.1 M KCl solution at the PAn/BBNs-20wt.% modified GCE for the cycle for the 1st and 20th time, respectively. Scan rate, 50 mVs^{-1}.

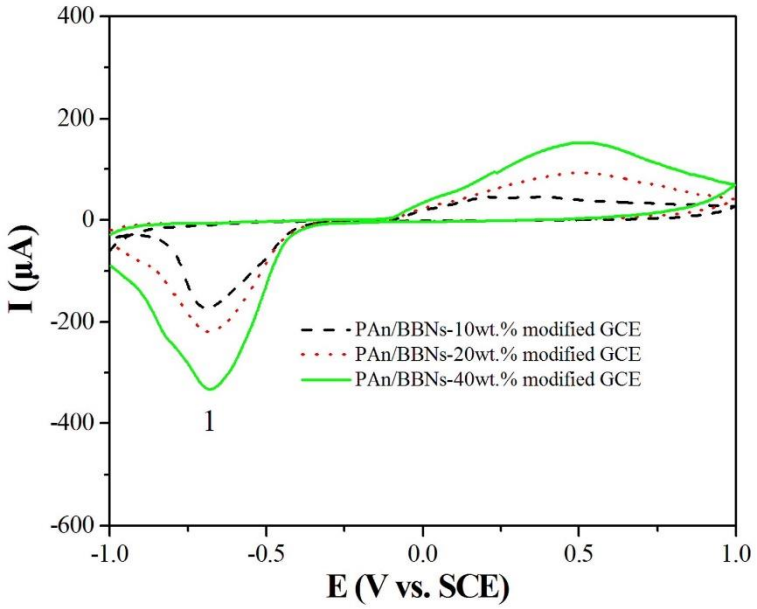

Figure 10. CVs of 2 mM TA in 0.1 M KCl solution at the PAn/BBNs modified GCEs with various PAn content. Scan rate, 50 mVs^{-1}.

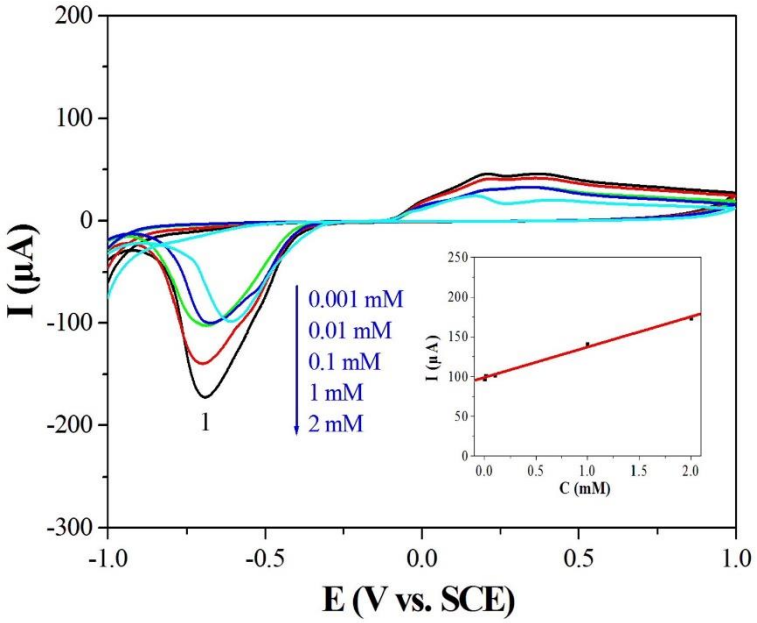

Figure 11. CVs of TA with various concentrations in 0.1 M KCl solution at the PAn/BBNs-10wt.% modified GCE. Scan rate, 50 mVs^{-1}. The inset in the bottom-right part is the plot of the current of the CV peak against TA concentration.

When the PAn/BBNs-20wt.% modified GCE was stored under the air atmosphere for 2 weeks, there is only slight difference in the current response indicating good long-term stability of the composites modified GCE. Twenty recycling measurements in the mixed solution of 0.1 KCl and 2 mM TA were used to analyse the reproducibility of the PAn/BBNs modified GCE. Figure 9 shows the CVs of 2 mM TA in 0.1 M KCl solution at the composites modified GCE for the 1st and 20th time, respectively using same PAn/BBNs-20wt.% modified GCE. The relative standard deviation (R.S.D.) is

3.43%. Combining the above results, the PAn/BBNs modified GCE shows great application potential for electrochemical sensor to detect TA.

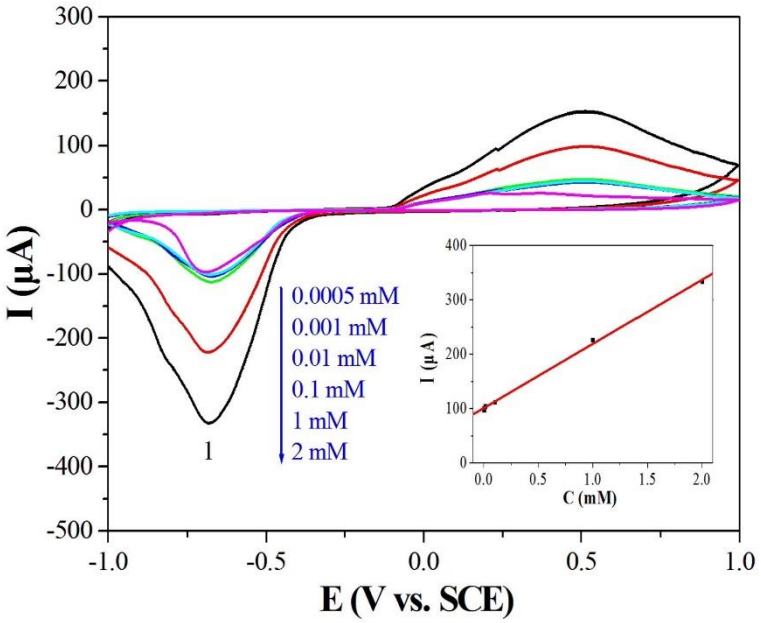

Figure 12. CVs of TA with various concentrations in 0.1 M KCl solution at the PAn/BBNs-40wt.% modified GCE. Scan rate, 50 mVs^{-1}. The inset in the bottom-right part is the plot of the current of the CV peak against TA concentration.

The electrochemical responses of the PAn/BBNs modified GCEs with different PAn mass percentage (Figure 10) were obtained to analyse the role of the PAn. Comparing the electrochemical responses of the Ba bismuthate nanobelts modified GCE, the current of the CV peak cvp1 increases from 174.1 μA to 333.2 μA with the PAn mass percentage from 10wt.% to 40wt.%. The larger peak current shows the improved electrochemical activity toward TA. LOD, linear range and correlation coefficient R using the PAn/BBNs modified GCEs with different PAn mass percentages were also analyzed. The CVs of 2 mM TA in 0.1 M KCl solution at the composites modified GCE are shown in Figure 11 and Figure 12. It is obvious that the peak current increases with the TA concentration.

Table 2. Analytical data of TA at the PAn/BBNs-10wt.% and PAn/BBNs-40wt.% modified GCEs.

CV peak	Regression equation[a]	Correlation coefficient (R)	Linear range (mM)	LOD (μM) [b]	PAn mass percentage (wt.%)
Cvp1	I_p=101.448+37.131C	0.997	0.001-2	0.1	10
Cvp1	I_p=111.408+112.141C1 37C	0.999	0.0005-2	0.08	40

[a] Where I_p and C refer to the CV peak current (μA) and TA concentration (mM)
[b] The LOD was calculated using S/N=3

Table 2 indicates the analytical results using the PAn/BBNs-10wt.% and PAn/BBNs-40wt.% modified GCE, respectively. The linear range increases from 0.001-2 mM to 0.0005-2 mM. LOD decreases from 0.12 μM to 0.08 μM with increasing the polyaniline mass percentage from 10% to 40%. The PAn/BBNs-40wt.% composites show the best electrochemical performance for TA detection. Table 3 shows the comparison data for TA determination using different electrodes and methods. The PAn/BBNs-40wt.% modified GCE has the LOD of 0.08 μM for TA detection which is far lower than that using other electrodes. And the linear range is also wider. Therefore, the PAn/BBNs modified GCE shows wide linear range and low LOD. Polyaniline enhances the electrochemical performance for TA owing to electrochemically active performance and synergistic role between the polyaniline and Ba bismuthate nanobelts.

Table 3. Comparison data for TA determination using different electrodes and methods.

Electrodes and methods	Linear range (mM)	LOD (μM)	References
Aluminium bismuthate nanorods modified GCE, Electrochemical method	0.001-2	0.64	8
Ba bismuthate nanobelts modified GCE, Electrochemical method	0.001-2	0.12	10
Cobalt(II)-phthalocyanine modified carbon paste electrode, Electrochemical method	0.01-0.1	7.29	12
Cu bismuthate nanosheets modified GCE, Electrochemical method	0.005-2	1.4	33
Carbon electrode, C-13 NMR spectroscopy	—	300	34
Bismuth nickelate nanorods modified GCE, Electrochemical method	0.001-2	0.52	35
Calcium vanadate nanorods modified GCE, Electrochemical method	0.005-2	2.4	36
PAn/BBNs-40wt.% modified GCE, Electrochemical method	0.0005-2	0.08	This work

4. CONCLUSIONS

In summary, PAn/BBN composites with different polyaniline mass percentages have been obtained by an *in-situ* polymerization process and the electrochemical behaviors for TA at the PAn/BBN composites modified GCE have been investigated. The amorphous polyaniline nanoscale particles with the size of less than 100 nm attach to the surface of the crystalline Ba bismuthate nanobelts. The PAn/BBNs-20wt.% composites modified GCE exhibits good electro-catalytic activity toward TA with a wide linear range and LOD of 0.0005-2 mM and 0.09 μM, respectively. LOD decreases from 0.12 μM to 0.08 μM with increasing the polyaniline mass percentage from 10% to 40%. The PAn/BBN composites modified GCE shows enhanced electro-catalytic activity toward TA

with good stability and reproducibility. The PAn/BBNs modified GCE shows great application potential for electrochemical sensor to detect TA.

ACKNOWLEDGMENTS
This work was supported by the Major Scientific Instrument Development Project of National Natural Science Foundation of China (No. 41627801) and Student Innovation and Entrepreneurship Training Program of P.R. China (201810360023, 201910360014, 201910360018).

References

1. S. Arlt, J. Harloff, A. Schulz, A. Stoffers and A. Villinger, *Inorg. Chem.*, 55 (2016) 12321.
2. T. X. Fu, *Mater. Res. Bull.*, 99 (2018) 460.
3. S. Y. Cao, C. S. Chen, X. D. Xi, B. Zeng, X. T. Ning, T. G. Liu, X. H. Chen, X. M. Meng and X. M. Xiao, *Vacuum*, 102 (2014) 1.
4. H. Sopha, L. Baldrianová, E. Tesařová, G. Grincienė, T. Weidlich, I. Švancara and S. B. Hočevar, *Electroanal.*, 22 (2010) 1489.
5. Y. Z. Sun, M. Yang, J. Q. Pan, P. Y. Wang, W. Li, and P. Y. Wan, *Electrochim. Acta*, 197 (2016) 68.
6. A. Padmanaban, T. Dhanasekaran, R. Manigandan, S. P. Kumar, G. Gnanamoorthy, A. Stephen and V. Narayanan, *New. J. Chem.*, 41 (2017) 7020.
7. L. Z. Pei, T. Wei, N. Lin, Z. Y. Cai, C. G. Fan and Z. Yang, *J. Electrochem. Soc.*, 163 (2016) H1.
8. L. Z. Pei, T. Wei, N. Lin, C. G. Fan and Z. Yang, *J. Alloys Compd.*, 679 (2016) 39.
9. L. Z. Pei, T. Wei, N. Lin, H Zhang and C. G. Fan, *Russ. J. Electrochem.*, 54 (2018) 84.
10. L. Z. Pei, F. F. Lin, F. L. Qiu, W. L. Wang, Y. Zhang and C. G. Fan, *Mater. Res. Express*, 4 (2017) 075047.
11. K. Zawada, A. Plichta, D. Jańczewski, H. Hajmowicz, Z. Florjańczyk, M. Stepień, A. Sobiecka and L. Synoradzki, *ACS Sustainable Chem. Eng.*, 5 (2017) 5999.
12. A. S. Lourenco, R. F. Nascimento, A. C. Silva, W. F. Ribeiro, M. C. U. Araujo, S. C. B. Oliveira and V. B. Nascimento, *Anal. Chim. Acta*, 1008 (2018) 29.
13. L. M. Likhosherstov, O. S. Novikova, N. G. Kolotyrkina, B. B. Berezin and V. E. Piskarev, *Russ. Chem. Bull.*, 67 (2018) 371.
14. H. Zhang, Y. S. Wang, D. W. Zhao, D. D. Zeng and J. Y. Xia, *ACS Appl. Mater. Interf.*, 7 (2015) 16152.
15. W. W. Yu, X. A. Chen, W. Mei C. S. Chen and Y. H. Tsang, *Appl. Surf. Sci.*, 400 (2017) 129.
16. J. F. Duan, C. Zhu, Y. H. Du, Y. L. Wu, Z. Y. Chen, L. J. Li, H. L. Zhu and Z. Y. Zhu, *J. Mater. Sci.*, 52 (2017) 10470.
17. C. S. Chen, W. W. Yu, T. G. Liu, S. Y. Cao and Y. H. Tsang, *Sol. Energ. Mat. Sol. C.*, 160 (2017) 43.
18. S. Hussain, E. Kovacevic, R. Amade, J. Bemdt, C. Pattyn, A. Dias, C. Boulmer-Leborgne, M. R. Ammar and E. Bertran-Serra, *Electrochim. Acta*, 268 (2018) 218.
19. S. K. Kandasamy and K. Kandasamy, *J. Inorg. Organomet. Polym. Mater.*, 28 (2018) 559.
20. J. Li, H. Xie, Y. Li, J. Liu and Z. Li, *J. Power Sources*, 193 (2011) 10775.
21. Y. K. Zhou, B. L. He, W. J. Zhou, J. E. Huang, X. H. Li, B. Wu and H. L. Li, *Electrochim. Acta*, 49 (2004) 257.
22. J. Hu, H. Wang and X. Huang, *Electrochim. Acta*, 74 (2012) 98.
23. K. J. Huang, J. Z. Zhang, Y. J. Liu and L. L. Wang, *Sens. Actuat. B: Chem.*, 194 (2014) 303.
24. W. Z. Huang, X. Y. Gan and L. Zhu, *Ceram. Int.*, 44 (2018) 5473.
25. G. Zheng, J. Wu, W. Wang and C. Pan, *Carbon*, 42 (2004) 2839.

26. Y. Z. Liao, C. Zhang, Y. Zhang, V. Strong, J. S. Tang, X. G. Li, K. Kalantar-zadeh, E. M. V. Hoek, K. L. Wang and R. B. Kaner, *Nano Lett.*, 11 (2011) 954.
27. L. Z. Pei, Y. Ma, F. L. Qiu, F. F. Lin, C. G. Fan and X. Z. Ling, *Mater. Res. Express*, 6 (2019) 015053.
28. L. Z. Pei, F. L. Qiu, Y. Ma, F. F. Lin, C. G. Fan, X. Z. Ling and S. B. Zhu, *Fuller. Nanotub. Car. N.*, 27 (2019) 58.
29. L. Z. Pei, H. D. Liu, N. Lin, Y. K. Xie and Z. Y. Cai, *Curr. Pharm. Anal.*, 11 (2019) 16.
30. Z. W. Lu, W. L. Dai, B. C. Liu, G. Q. Mo, J. J. Zhang, J. P. Ye and J. S. Ye, *J. Colloid Interf. Sci.*, 525 (2018) 86.
31. N. Wang, P. R. Chang, P. W. Zheng and X. F. Ma, *Diam. Relat. Mater.*, 55 (2015) 117.
32. Z. Y. Cai, F. F. Lin, T. Wei, D. G. Fu and L. Z. Pei, *Int. J. Electrochem. Sci.*, 14 (2019) 4371.
33. Y. Zhang, F. F. Lin, T. Wei and L. Z. Pei, *J. Alloy. Compd.*, 723 (2017) 1062.
34. A. Rapp, A. Markowetz, M. Spraul and E. Humpfer, *Fresenius'Z. Anal. Chem.*, 330 (1988) 462.
35. L. Z. Pei, T. Wei, N. Lin and H. Zhang, *J. Alloy. Compd.*, 663 (2016) 677.
36. L. Z. Pei, Y. Q. Pei, Y. K. Xie, C. G. Fan, D. K. Li and Q. F. Zhang, J. Mater. Res., 27 (2012) 2391.